

---

# BET-HEDGING STRATEGIES IN EXPANDING POPULATIONS

---

A PREPRINT

**Paula Villa Martín**

Biological Complexity Unit,  
Okinawa Institute of Science and Technology Graduate University,  
Onna, Okinawa 904-0495, Japan

**Miguel A. Muñoz**

Departamento de Electromagnetismo y Física de la Materia  
and Instituto Carlos I de Física Teórica y Computacional,  
Universidad de Granada, Granada, Spain

**Simone Pigolotti**

Biological Complexity Unit,  
Okinawa Institute of Science and Technology Graduate University,  
Onna, Okinawa 904-0495, Japan  
simone.pigolotti@oist.jp

January 27, 2022

## ABSTRACT

In ecology, species can mitigate their extinction risks in uncertain environments by diversifying individual phenotypes. This observation is quantified by the theory of bet-hedging, which provides a reason for the degree of phenotypic diversity observed even in clonal populations. The theory of bet-hedging in well-mixed populations is rather well developed. However, many species underwent range expansions during their evolutionary history, and the importance of phenotypic diversity in such scenarios still needs to be understood. In this paper, we develop a theory of bet-hedging for populations colonizing new, unknown environments that fluctuate either in space or time. In this case, we find that bet-hedging is a more favorable strategy than in well-mixed populations. For slow rates of variation, temporal and spatial fluctuations lead to different outcomes. In spatially fluctuating environments, bet-hedging is favored compared to temporally fluctuating environments. In the limit of frequent environmental variation, no opportunity for bet-hedging exists, regardless of the nature of the environmental fluctuations. For the same model, bet-hedging is never an advantageous strategy in the well-mixed case, supporting the view that range expansions strongly promote diversification. These conclusions are robust against stochasticity induced by finite population sizes. Our findings shed light on the importance of phenotypic heterogeneity in range expansions, paving the way to novel approaches to understand how biodiversity emerges and is maintained.

**Keywords** Population dynamics · Environmental variability · Range expansion · Fisher waves

## 1 Introduction

The dynamics and evolutionary history of many biological species, from bacteria to humans, are characterized by invasions and expansions into new territory. The effectiveness of such expansions is crucial in determining the ecological range and therefore the success of a species. A large body of observational [Ramachandran et al., 2005, Duckworth, 2008] and experimental [Wolfe and Berg, 1989, Hallatschek et al., 2007, Mayor and Etienne-Manneville, 2016, Fu et al., 2018] literature indicates that evolution and selection of species undergoing range expansions can be dramatically different from that of other species resident in a fixed habitat. Theoretical studies of range expansions based on the Fisher-Kolmogorov equation [Fisher, 1937, Kolmogorov et al., 1937] or variants [Neubert and Caswell, 2000, Bartoń et al., 2012] also support this idea. Adaptive dispersal strategies [Duckworth, 2008] and small population sizes at the edges of expanding fronts [Waters et al., 2013, Hallatschek and Nelson, 2008] are among the main reasons for such differences.

Range expansions often occur in non-homogeneous and fluctuating environments. Under such conditions, it is possible to mathematically predict the expansion velocity of a community of phenotypically identical individuals [Shigesada et al., 1979, 1986, Shigesada and Kawasaki, 1997, Hastings et al., 2005, Schreiber and Lloyd-Smith, 2009, Dewhurst and Lutscher, 2009]. However, diversity among individuals is expected to play an important positive role when populations expand in fluctuating environments. For instance, diverse behavioral strategies help animal populations to overcome different invasion stages and conditions [Wolf and Weissing, 2012, Sih et al., 2012, Chapple et al., 2012, Carere and Gherardi, 2013]. Analyses of phenotypic diversity in motile cells suggest that it also may lead to a selective advantage at a population level [Frankel et al., 2014, Dufour et al., 2014, 2016]. Although several studies have tackled the problem of how individual variability affects population expansion [Neubert and Caswell, 2000, Bartoń et al., 2012, Fogarty et al., 2011, Fu et al., 2018, Ben-Jacob et al., 2000, Keller and Segel, 1971, Ben-Jacob et al., 2000, Lin and Wang, 2014, Emako et al., 2016], systematic and predictive theory is still lacking [Carere and Gherardi, 2013].

Phenotypic diversification is often interpreted as a bet-hedging strategy, spreading the risk of uncertain environmental conditions across different phenotypes adapted to different environments [Veening et al., 2008, Kussell and Leibler, 2005, Wolf et al., 2005a,b, Solopova et al., 2014, Stumpf et al., 2002, Rouzine et al., 2015, Childs et al., 2010, Hidalgo et al., 2016, Hopper, 1999]. Since its formalization in the context of information theory and portfolio diversification [Kelly Jr, 2011, Fernholz and Shay, 1982], a large number of works have explored the applicability of bet-hedging in evolutionary game theory [Smith, 1988, Nowak, 2006, Harmer and Abbott, 1999, Parrondo et al., 2000] and ecology [de Jong et al., 2011, Williams and Hastings, 2011, Comins et al., 1980, Hamilton and May, 1977, Jansen and Yoshimura, 1998]. Few studies have explored the benefits of bet-hedging in spatially structured ecosystems [Hidalgo et al., 2015, Rajon et al., 2009].

In this paper, we study how bet-hedging strategies can aid populations in invading new territories characterized by fluctuating environments. In particular, we analyze the effect of spatial expansion, different types of environmental heterogeneity, and demographic stochasticity on development of bet-hedging strategies for a population front evolving according to a Fisher wave.

By employing mathematical as well as extensive computational analyses, we find that the advantage of bet-hedging in range expansions depends on the rate of environmental variation. In particular, bet-hedging is more convenient for infrequently varying environments, whereas its advantages vanish for frequent environmental variation. For the same model, bet-hedging is never an advantageous strategy in the well-mixed case, supporting the view that range expansions strongly promote diversification. We further find that spatial environmental variations provide more opportunities for bet-hedging than temporal fluctuations. Finally, we show that our conclusions still hold when considering stochastic effects on the front propagation induced by a finite population size.

The paper is organized as follows. In Section 2 we introduce a general population model and an example with two available phenotypes and two environmental states. Section 3.1 presents an extensive study of this example. In 3.2, we demonstrate that the main conclusions obtained for the example also hold for the general model. Section 4 is devoted to conclusions and perspectives.

## 2 Model

We consider a population consisting of individuals that can assume  $N$  alternative phenotypes. The population as a whole adopts a phenotypic strategy, that is identified by the fractions  $\alpha_i$ ,  $i = 1 \dots N$  of the population assuming each phenotype  $i$  with  $\sum_i \alpha_i = 1$  and  $0 \leq \alpha_i \leq 1 \forall i$  (Fig. 1A). As customary in game theory, we say that a strategy is a “pure strategy” if  $\alpha_i = \delta_{ik}$  for some phenotype  $k$ , and a “mixed strategy” otherwise. We assume that the  $\alpha_i$ ’s remain constant in time within the population.

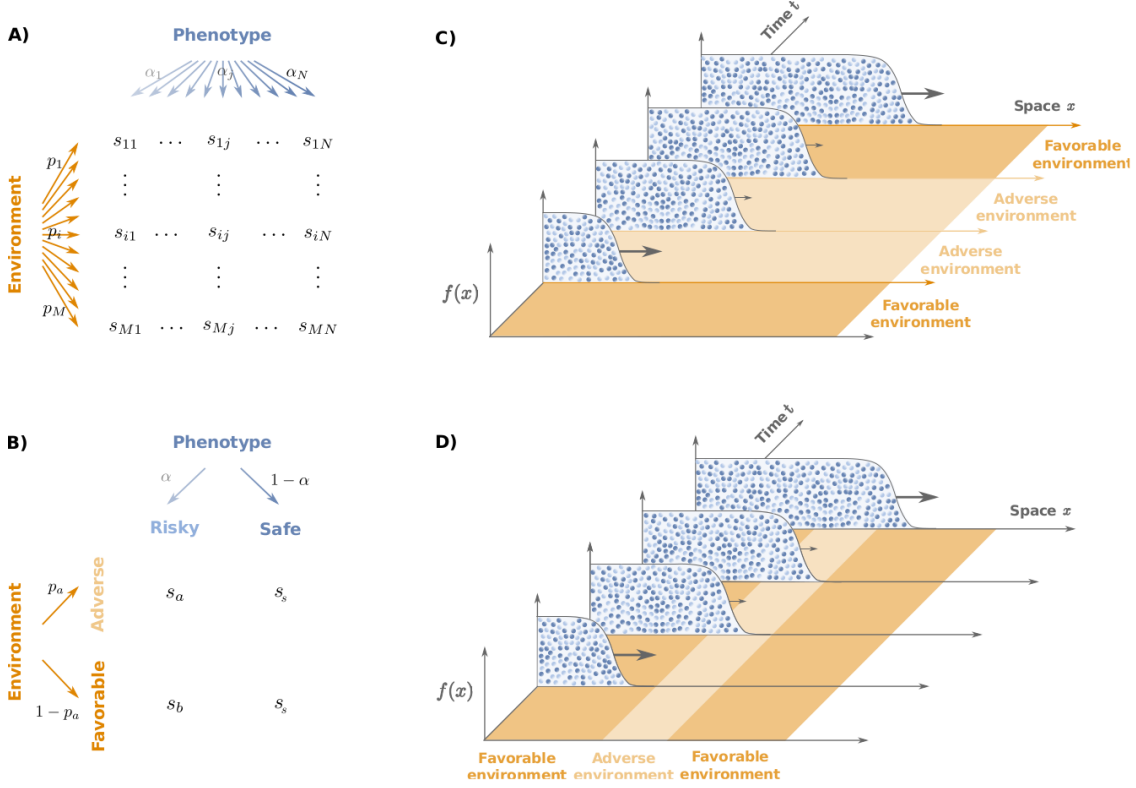


Figure 1: **Population model.** A) General model: individuals can adopt  $N$  different phenotypes with probabilities  $\alpha_j$  ( $j = 1, \dots, N$ ) and experience  $M$  different environmental conditions with probabilities  $p_i$  ( $i = 1, \dots, M$ ). The fitness of an individual with phenotype  $j$  in an environment  $i$  is given by  $s_{ij}$ . B) Two-phenotypes model: Individuals can adopt either a “risky” or a “safe” phenotype with probabilities  $\alpha$ , and  $1 - \alpha$  respectively. The safe phenotype is characterized by an environment-independent growth rate  $s_s$ . The growth rate of the risky phenotype is  $s_a$  or  $s_b$ , depending on whether the current environment is “adverse” (a) or “favorable” (b). C) and D) Sketch of range expansion in a population having  $0 \leq \alpha \leq 1$  for temporally varying C) and spatially varying D) environments, respectively.

The environment can be found in one of  $M$  different states, which can randomly alternate either in time or in space. We call  $p_i$  the probability of encountering environment  $i$ . We further define the growth rate  $s_{ij} \geq 0$  of phenotype  $j$  in environment  $i$  (Fig. 1A). When the population size is sufficiently large, so that demographic stochasticity can be neglected, the population-averaged growth rate given the state  $i = i(x, t)$  of the environment at position  $x$  and time  $t$  is

$$\sigma_i = \sum_j \alpha_j s_{ij}. \quad (1)$$

Since Eq. 1 is linear in the  $\alpha_j$ 's, the population-averaged growth rate in a given environment is always maximized by the pure strategy with the highest growth rate. However, in the presence of uncertainty about the environment, the population might choose other strategies. One possibility is to select a different pure strategy, less risky than the optimal one. This case is often termed “conservative bet-hedging” in the ecological literature [Hopper, 1999]. Another option is to adopt a mixed strategy, with different phenotypes more adapted to different environments. This case is termed “diversifying bet-hedging” in the literature [Den Boer, 1968, Hopper, 1999]. Since our interest is in diversification, the term “bet-hedging” will refer herein to diversifying bet-hedging.

Before presenting our results in full generality, we will illustrate it in a simple, yet ecologically relevant instance of the model with only two phenotypes: “safe” and “risky” and two environmental states: “adverse” (a) and “favorable” (b). The safe phenotype is characterized by a growth rate  $s_s$  both in the adverse and favorable environments. The growth rate of the risky phenotype is  $s_a$  in environment (a) and  $s_b$  in environment (b) (Fig. 1B) [Hufton et al., 2018]. The two environments occur with the same probability,  $p_a = p_b = 1/2$ . A fraction of individuals  $\alpha$  adopts the risky phenotype

and the complementary fraction  $(1 - \alpha)$  adopts the safe phenotype (Fig. 1B). For this model, the population-averaged growth rate reads

$$\sigma(x, t) = \begin{cases} \sigma_a = (1 - \alpha)s_s + \alpha s_a, & \text{in env. a} \\ \sigma_b = (1 - \alpha)s_s + \alpha s_b. & \text{in env. b} \end{cases} \quad (2)$$

Note that, with a slight abuse of notation, we use equivalently  $\sigma_i$  or  $\sigma(x, t)$  to denote the population-averaged growth rate in the environment  $i(x, t)$ . For pure strategies,  $\alpha = 0$  or  $\alpha = 1$ , the population-averaged growth rate  $\sigma$  reduces to the growth rate of the safe or risky phenotype, respectively.

### 3 Results

#### 3.1 Two-phenotype model

We seek to understand those conditions under which bet-hedging is advantageous for the population. To this end, we shall compare three situations: i) well-mixed populations, ii) range expansions in environments that fluctuate temporally, but that are homogeneous in space (Fig. 1C), and iii) range expansions in spatially fluctuating environments that are homogeneous in time (Fig. 1D).

##### 3.1.1 Well-mixed case

We start by analyzing the well-mixed case, where the spatial coordinates of individuals can be ignored. The total population density  $f(t)$  evolves according to the equation

$$\frac{d}{dt}f(t) = \sigma(t)f(t). \quad (3)$$

In writing Eq. 3, we used the assumption that the fraction  $\alpha$  of the population adopting the risky phenotype remains constant in time (see [Ashcroft et al., 2014, Hufton et al., 2016] for cases in which this assumption is relaxed). Equation 3 can be readily integrated, obtaining

$$\ln \left( \frac{f(t)}{f(0)} \right) = \int_0^t dt' \sigma(t') \xrightarrow{t \gg 1} t \langle \sigma_i \rangle \quad (4)$$

where  $\langle \sigma_i \rangle = \sum_i p_i \sigma_i$  denotes an average over the environmental states. For Eq. 4 to hold, we do not need to make strong assumptions about the statistics of the environmental states, other than it should be stationary, ergodic, and with a finite correlation time.

The optimal strategy  $\alpha^*$  is obtained by maximizing the right-hand side of Eq. 4 respect to the strategy  $\alpha$ . Since  $\langle \sigma_i \rangle$  is a linear function of  $\alpha$ , its maximum is always reached at the extremes of the interval ( $\alpha \in [0, 1]$ ). In particular, defining the normalized growth rates  $\tilde{s}_a \equiv s_a/s_s$  and  $\tilde{s}_b \equiv s_b/s_s$ , we find that the optimal strategy is  $\alpha^* = 1$  when  $\tilde{s}_b > 2 - \tilde{s}_a$  and  $\alpha^* = 0$  otherwise. This means that no bet-hedging strategy is possible in this model in the well-mixed case [Hufton et al., 2018].

This simple result illustrates an aspect of bet-hedging that is sometimes under-appreciated. In well-mixed systems, bet-hedging optimal strategies appear when the model includes at least one of the following ingredients: a) discrete generations, as in the seminal work of Kelly [Kelly Jr, 2011], b) finite switching rates among strategies [Kussell and Leibler, 2005, Hufton et al., 2016], or c) a delta-correlated environment [Hidalgo et al., 2015]. Any of these ingredients can lead to nonlinearities in the average exponential growth rate, therefore opening the way for a non-trivial optimal strategy.

Note that, in this model, the frequency of environmental change does not play a role, as far as it is finite [Hidalgo et al., 2015]. The physical reason can be understood from the right-hand side of Eq. 4: the optimal strategy depends on the frequency of different environmental states but not on the switching rates. This feature is also shared by other well-mixed models that do allow for optimal bet-hedging strategies, such as the classic model by Kelly [Kelly Jr, 2011]. We shall see in the following that, on the contrary, the rate of environmental change plays an important role for expanding populations.

### 3.1.2 Range expansion in fluctuating environments

We now consider a population expanding into an unoccupied, one-dimensional space under the influence of a stochastically changing environment. Its population dynamics are described by the Fisher equation [Fisher, 1937, Van Saarloos, 2003]:

$$\partial_t f(x, t) = D \nabla^2 f(x, t) + \sigma(x, t) f(x, t) (1 - f(x, t)), \quad (5)$$

where  $f(x, t)$  is the population density at spatial coordinate  $x$  and time  $t$ , and  $D$  is the diffusion constant, which characterizes the motility of individuals. For a constant growth rate  $\sigma$ , the stationary solution of Eq. 5 is characterized by a front advancing in space with velocity  $v_F = 2\sqrt{D\sigma}$ . Instead, we consider a fluctuating case in which the growth rate  $\sigma(x, t)$  depends on the population strategy  $\alpha$  and on environmental conditions according to Eq. 2. In such case, one can define an asymptotic mean velocity of the front as

$$v_M = \lim_{t \rightarrow \infty} \frac{1}{t} \int_0^\infty f(x, t) dx. \quad (6)$$

In what follows, we take  $v_M$  as a proxy of the long-term population fitness and maximize it with respect to  $\alpha$  to determine the optimal strategy.

### 3.1.3 Range expansion in temporally varying environments

We first consider the case in which environmental conditions change randomly with time, but are homogeneous across space,  $\sigma(x, t) = \sigma(t)$  (see Fig. 1C). Switching rates between adverse and favorable environments are  $k_{a \rightarrow b} = k_{b \rightarrow a} = k$ . We first estimate the asymptotic mean velocity defined in Eq. 6 in the limiting cases of  $k \rightarrow 0$  and  $k \rightarrow \infty$ .

When the environment changes very infrequently,  $k \rightarrow 0$ , the population front has the time to relax to the asymptotic shape characterized by its corresponding Fisher velocity,  $v_a = 2\sqrt{D\sigma_a}$  or  $v_b = 2\sqrt{D\sigma_b}$  depending on the environment [Fisher, 1937, Cencini et al., 2003]. Thus, the asymptotic mean velocity can be estimated as  $v_M = (v_a + v_b)/2$ . Maximizing  $v_M$  with respect to  $\alpha$ , we find that in this case, a bet-hedging optimal strategy exists under the conditions (Fig. 2A):

$$\begin{aligned} \tilde{s}_b &> 2 - \tilde{s}_a, \\ \tilde{s}_b &< 1/\tilde{s}_a. \end{aligned} \quad (7)$$

In the opposite limiting case of a rapidly fluctuating environment,  $k \rightarrow \infty$ , the population effectively experiences the average of the two growth rates, so that the velocity can be estimated as  $v_M \approx 2\sqrt{D\langle\sigma\rangle}$ , where  $\langle \dots \rangle$  denotes an average over the environmental states. In this case, the optimal strategy  $\alpha^*$  is achieved by maximizing the average growth rate  $\langle \sigma \rangle$  with respect to  $\alpha$ . Since  $\langle \sigma \rangle$  is linear in  $\alpha$ , the maximum always lies at the extremes of the interval  $[0, 1]$ . In particular, we find  $\alpha^* = 1$  when  $\tilde{s}_b > 2 - \tilde{s}_a$  and  $\alpha^* = 0$  otherwise, as in the well-mixed case. This implies that no bet-hedging regime exists in this limit (Fig. 2B).

To explore the intermediate regimes of finite  $k$ , it is necessary to resort to numerical simulations of Eq. 5. For a set of parameters such that the optimal strategy is  $\alpha^* = 1$  for  $k \rightarrow 0$ , the optimal strategy remains  $\alpha^* = 1$  for all values of  $k$ , see Fig. 3A. Instead, in a case where the optimal solution is in the bet-hedging region for  $k \rightarrow 0$ , the optimal strategy  $\alpha^*$  increases with the switching rate, so that for large  $k$  the optimal strategy is outside the bet-hedging region,  $\alpha^* = 1$ . These results support our analytical estimates of limiting values and suggest that the asymptotic mean velocity is a monotonically increasing function of the switching rate  $k$  in this case.

### 3.1.4 Range expansion in spatially varying environments

We now consider the case in which environmental conditions are constant in time, but depend on the spatial coordinate  $x$ . The dynamics are described by the Fisher equation 5 with two types of environment randomly alternating in space,  $\sigma(x, t) = \sigma(x)$ . We call  $k_S$  the spatial rate of environmental switch, so that the probability of encountering an environmental shift within an infinitesimal spatial interval  $dx$  is equal to  $k_S dx$ . The switching rates from environment  $a$  to  $b$  and vice-versa are both equal to  $k_S$ . As above, we first analyze the two limits  $k_S \rightarrow 0$  and  $k_S \rightarrow \infty$ .

In the limit  $k_S \rightarrow 0$ , the population front traverses large regions of space characterized by a constant environment, either  $a$  or  $b$ , thus being able to reach the corresponding Fisher velocity,  $v_a$  or  $v_b$ , respectively. The mean traversed lengths  $\Delta x_a$  and  $\Delta x_b$  are equal for the two environments. On the other hand, the mean times spent in each of them,  $t_a$  and  $t_b$ , are different, and satisfy the relation

$$\frac{t_a}{t_b} = \frac{\Delta x_a/v_a}{\Delta x_b/v_b} = \frac{v_b}{v_a}. \quad (8)$$

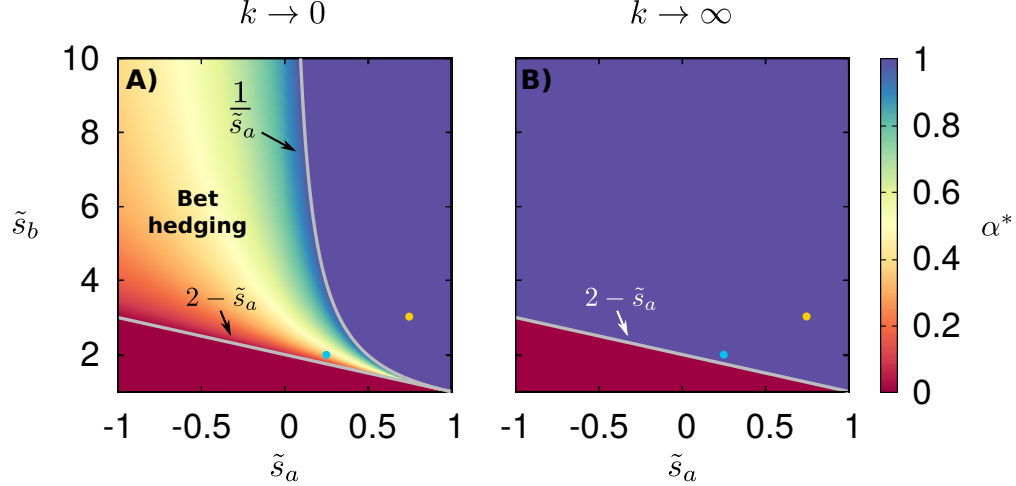


Figure 2: **Bet-hedging region in temporally varying environments** Optimal strategy  $\alpha^*$  as a function of growth rates  $\tilde{s}_a \equiv s_a/s_s$  and  $\tilde{s}_b \equiv s_b/s_s$  for range expansions in temporally varying environments under the limits of environmental change rate (A)  $k \rightarrow 0$ , see Eq.7, and (B)  $k \rightarrow \infty$ . In all panels, lines delimit the bet-hedging region  $0 \leq \alpha^* \leq 1$ . Two dots in the panels mark parameter values chosen for the analysis of Figs. 3,4,5.

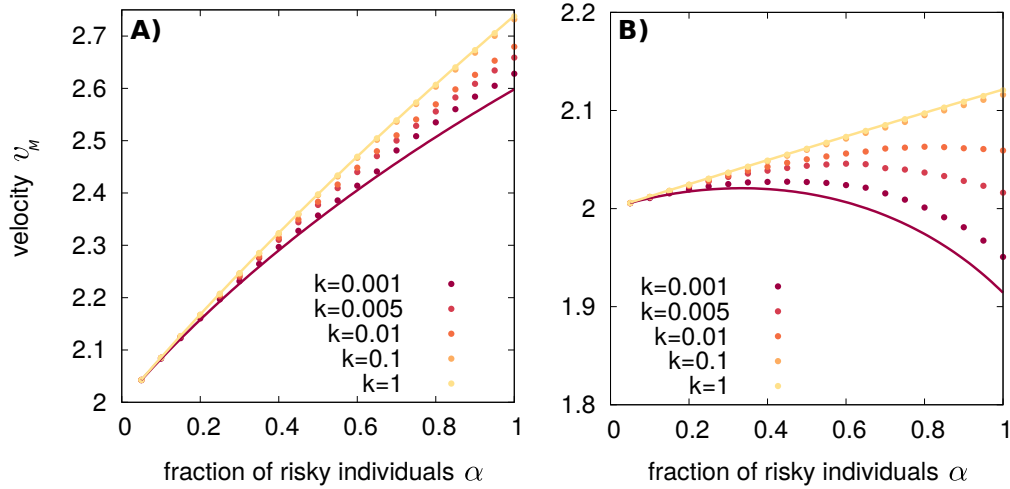


Figure 3: **The asymptotic mean velocity increases with  $k$  in temporally varying environments.** (A) Velocities obtained by numerical integration of Eq. 5 for  $s_a = 0.75$ ,  $s_s = 1$ ,  $s_b = 3$  (yellow dot of Fig. 2) for different switching rates  $k$  shown in the figure legend. (B) The same for  $s_a = 0.25$ ,  $s_s = 1$ ,  $s_b = 2$  (blue dot of Fig. 2). In (A), the optimal strategy is  $\alpha = 1$  for all  $k$  values. In (B), bet-hedging optimal strategies appear depending on the value of  $k$ . The continuous red and yellow lines (both in A and B) illustrate analytical predictions under the two limits  $v_M(k \rightarrow 0) = (v_a(\alpha) + v_b(\alpha))/2$  and  $v_M(k \rightarrow \infty) = 2\sqrt{D\langle\sigma(\alpha)\rangle}$ , respectively.

Therefore, in this case, the asymptotic mean velocity is given by the harmonic mean of the velocities in the two environments

$$v_M(k_S \rightarrow 0) = \frac{t_a v_a + t_b v_b}{t_a + t_b} = \frac{2v_a v_b}{v_a + v_b}. \quad (9)$$

At the opposite limit of large  $k_S$ , the environment is characterized by frequent spatial variations. In this case, the population front occupies multiple  $a$  and  $b$  sectors with an effective growth rate  $\langle\sigma\rangle$ . As in the time-varying case, the asymptotic mean velocity in this limit is  $v_M(k_S \rightarrow \infty) = 2\sqrt{D\langle\sigma\rangle}$ , see also [Shigesada et al., 1986, Shigesada and Kawasaki, 1997].

Here, for  $k_S \rightarrow 0$  the bet-hedging region is broader with respect to the temporally fluctuating environment for  $k \rightarrow 0$ , see Fig. 4A. For  $k_S \rightarrow \infty$ , the optimal strategy is the same as in Fig. 2C and there is no bet-hedging regime.

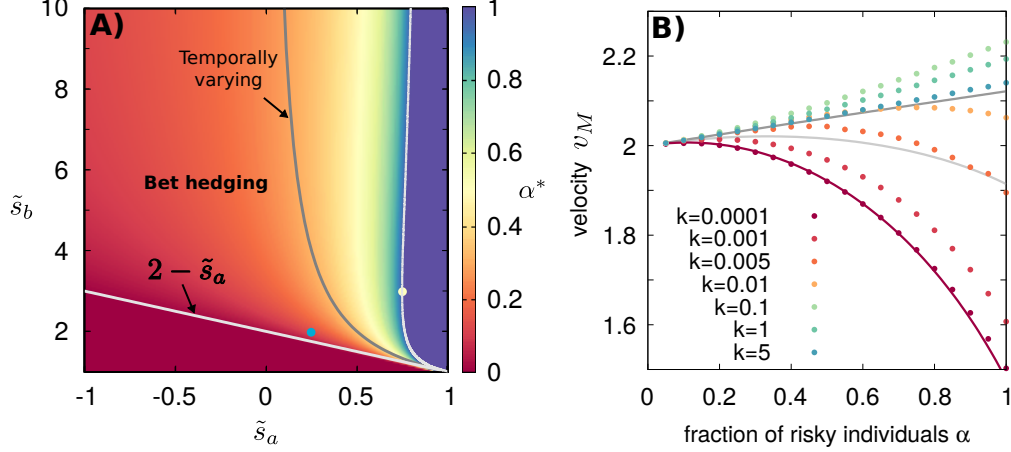


Figure 4: **The bet-hedging region is expanded for range expansions in spatially varying environments compared to temporally varying environments.** A) Optimal strategy  $\alpha^*$  as a function of the parameters for spatially varying environments in the limit  $k_S \rightarrow 0$ , Eq. 9. White lines mark the limits of the bet-hedging region. The limit for which the strategy  $\alpha = 1$  is optimal in temporally fluctuating environments for  $k \rightarrow 0$  is also shown (gray line) for comparison. B) The velocity obtained by numerical integration of Eq. 5 for  $s_a = 0.25$ ,  $s_s = 1$ ,  $s_b = 2$  (corresponding to the blue dot of panel A) and different values of  $k_S$  shown in the figure legend. Light and dark gray lines correspond to the analytical limits for temporally varying environments,  $v_M(k \rightarrow 0) = (v_a(\alpha) + v_b(\alpha))/2$ , and  $v_M(k \rightarrow \infty) = v_M(k_S \rightarrow \infty) = 2\sqrt{D\langle\sigma(\alpha)\rangle}$ , respectively. The red curve is the analytical solution for a spatially fluctuating environment with  $k_S \rightarrow 0$ , see Eq. 9. Note that in this case, the asymptotic mean velocity does not increase monotonically with  $k_S$  but is maximal at  $k_S \approx 0.1$ .

We numerically solved Eq. 5 for intermediate values of  $k_S$  and obtained the mean asymptotic velocities as a function of  $\alpha$ , see Fig. 4 B. Results support theoretical predictions in the limiting cases  $k_S \rightarrow 0$  and  $k_S \rightarrow \infty$ . In this case, we observe a non-monotonic behavior of  $v_M$  as a function of  $k_S$ , so that the maximum mean velocity is attained at an intermediate switching rate. An analytical explanation of this non-trivial effect goes beyond the scope of this work.

### 3.1.5 Effect of finite population size

The deterministic Fisher equation (5) is rigorously valid only in the limit of infinite local population sizes. We now explore the robustness of our results when considering stochasticity induced by the finite size of populations, i.e. “demographic noise”. We focus on the case of a front propagating in a temporally varying environment. To study finite population size, we solve numerically a stochastic counterpart of the Fisher equation

$$\dot{f}(x, t) = D\nabla^2 f + \sigma(t)f(1 - f) + \sqrt{\frac{2}{N}}f(1 - f)\xi(x, t), \quad (10)$$

see e.g. [Korolev et al., 2010]. In Eq. 10,  $\xi(x, t)$  is Gaussian white noise with  $\langle\xi(x, t)\rangle = 0$ ,  $\langle\xi(x, t)\xi(x', t')\rangle = \delta(x - x')\delta(t - t')$ . The parameter  $N$  represents the number of individuals per unit length corresponding to  $f(x, t) = 1$ . For large population sizes,  $N \gg 1$ , Eq. 10 reduces to Eq. 5. Numerical integration of Eq. 10 requires some care due to the fact that both noise and the deterministic terms go to zero as the absorbing states  $f(x, t) = 0$  and  $f(x, t) = 1$  are approached [Dornic et al., 2005, Moro, 2004]. A detailed description of our integration scheme is presented in the Supporting information.

For a Fisher wave propagating in a homogeneous environment, demographic noise leads to a reduced front velocity  $v$  with respect to the deterministic case [Brunet and Derrida, 2001, Van Saarloos, 2003, Moro, 2001, 2004]

$$(v - v_F) \sim -\frac{C}{\ln^2(N)} \quad (11)$$

where  $C$  is a constant,  $N$  is the maximum population size per unit length, and  $v_F = 2\sqrt{D\sigma}$  is the Fisher velocity in the absence of demographic noise. Asymptotic mean velocities for stochastic waves in temporally varying environments are shown in Fig. 5. Also in this case, small populations, subject to relatively strong demographic noise, propagate more slowly than large populations. In particular, curves at different values of  $N$  can be approximately rescaled using Eq. 11, assuming that  $C$  does not depend on  $\alpha$  (insets of Fig. 5). These results imply that the optimal strategy  $\alpha^*$  is

robust with respect to demographic noise, at least for moderately to relatively large values of  $N$ . The same scaling holds for spatially varying environments, but with mild deviations that seem to expand the bet-hedging region even further, compared with the infinite population size limit (see Supporting information).

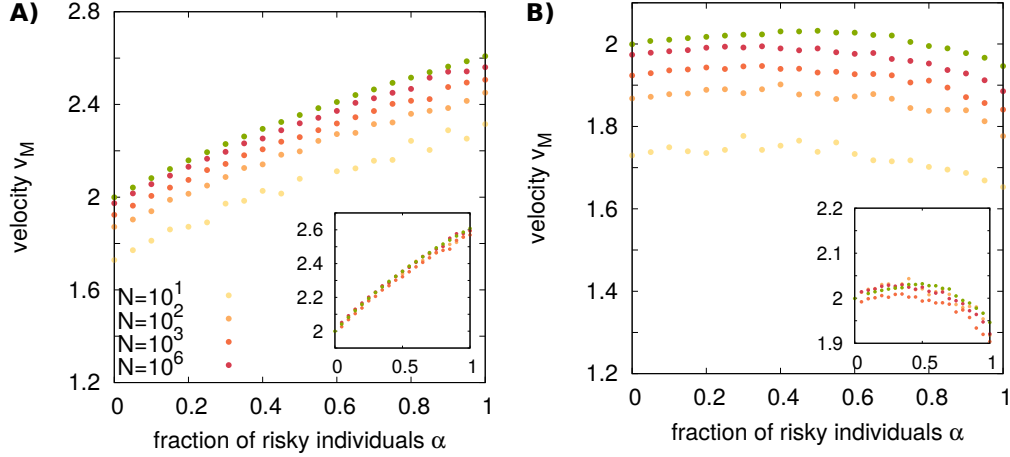


Figure 5: **The optimal strategy is robust with respect to noise induced by finite population size in temporally varying environments.** (A) Asymptotic mean velocities obtained by numerical integration of the stochastic Fisher equation 10 for  $\tilde{s}_a = 0.75$ ,  $s_s = 0.01$ ,  $\tilde{s}_b = 3$  (yellow dot of Fig. 2) and different population sizes. (B) The same for  $\tilde{s}_a = 0.25$ ,  $s_s = 1$ ,  $\tilde{s}_b = 2$  (blue dot of Fig. 2). In both panels, the temporal switching rate of the environment is  $k = 0.001$ . Green dots corresponds to the results of Figs. 3A,B for  $k = 0.001$ . Insets show a collapse of the curves according to Eq. 11, with a fitted value of  $C = 3$ .

### 3.2 General bet-hedging model

In this section, we demonstrate that our main conclusions hold also for the general case with  $N$  phenotypes and  $M$  environmental states (see Section 2). In particular, for a temporally fluctuating environment in the limit of very slow switching rates, the bet-hedging regime occupies a reduced region of parameter space compared to temporally constant environments fluctuating slowly in space. Also in this case, we find that for frequent environmental change, the propagation velocity tends to  $v_M \approx 2\sqrt{D\langle\sigma\rangle}$ , regardless of whether the environmental fluctuations depend on time or space. Therefore, the optimal strategy maximizes the linear function of the  $\alpha_i$ s  $\langle\sigma\rangle$  and is therefore a pure strategy as discussed after Eq. 1.

We consider a range expansion where the environment fluctuates in time and the stochastic switching rates among the  $M$  environmental states are small. Following the same line of thought of Section 3.1.3, the optimal strategy maximizes

$$\sigma_T = \frac{v_M(k \rightarrow 0)}{2\sqrt{D}} = \sum_i p_i \sqrt{\sigma_i} \quad (12)$$

where, as usual,  $\sigma_i = \sum_j s_{ij} \alpha_j$ . For spatially varying environments, the optimal strategy maximizes the harmonic mean

$$\sigma_S = \frac{v_F(k_S \rightarrow 0)}{2\sqrt{D}} = \frac{1}{\sum_i p_i \frac{1}{\sqrt{\sigma_i}}} \quad (13)$$

Both for Eq. 12 and Eq. 13, maximization has to be performed with the constraint  $\sum_j \alpha_j = 1$  and  $0 \leq \alpha_j \leq 1 \forall j$ . We recall that the bet-hedging regime is the region of parameter space where the optimal solution is a mixture of all phenotypes,  $\alpha_i > 0 \forall i$ . Here we show that if, for a given choice of the  $s_{ij}$ 's and  $p_i$ 's, a population advancing in a temporally varying environment is in a bet-hedging regime, then the same holds for spatially varying environments. For the demonstration, we borrow a mathematical tool from evolutionary game theory [Hofbauer and Sigmund, 1998]. We introduce the gradients



$$\begin{aligned}
F_l^T &= \frac{\partial \sigma^T}{\partial \alpha_l} = \left\langle \frac{s_l}{2\sqrt{\sigma}} \right\rangle \\
F_l^S &= \frac{\partial \sigma^S}{\partial \alpha_l} = (\sigma^S)^2 \left\langle \frac{s_l}{2\sigma^{3/2}} \right\rangle
\end{aligned} \tag{14}$$

where  $\langle x \rangle = \sum_i p_i x_i$  is the average over environments. We now associate replicator equations to Eq. 12 and Eq. 13:

$$\frac{d}{dt} \alpha_l = \alpha_l (F_l^T - \bar{F}^T) = \alpha_l \left\langle \frac{s_l - \sigma}{2\sqrt{\sigma}} \right\rangle \tag{15}$$

$$\frac{d}{dt} \alpha_l = \alpha_l (F_l^S - \bar{F}^S) = \alpha_l (\sigma^S)^2 \left\langle \frac{s_l - \sigma}{2\sigma^{3/2}} \right\rangle. \tag{16}$$

The system is in a bet-hedging regime when the replicator equations admit a stable fixed point in the interior of the unit simplex,  $0 < \alpha_i < 1$ . Instead of computing the fixed point explicitly, we check whether each phenotype  $l$  has a positive growth rate for  $\alpha_l \ll 1$ . Brouwer's fixed point theorem ensures that, under this condition, there must be a fixed point in the interior, see [Hofbauer and Sigmund, 1998], chapter 13. For our aims, it is therefore sufficient to prove that, for small  $\alpha_l$ , if  $(F_l^T - \bar{F}^T)$  is positive, then  $(F_l^S - \bar{F}^S)$  must be positive as well. Note that for  $\alpha_l \ll 1$ , the average  $\sigma = \sum_j s_{ij} \alpha_j$  does not depend on  $\alpha_l$ , and therefore,  $\sigma$  and  $s_l$  are uncorrelated random variables respect to the average over the environment. Since  $\sqrt{\sigma} > 0$ , this means that the sign of  $(F_l^T - \bar{F}^T)$  is the same than the quantity

$$\frac{1}{\langle \sqrt{\sigma} \rangle} \langle s_l \rangle \left\langle \frac{1}{\sqrt{\sigma}} \right\rangle - 1. \tag{17}$$

Following the same logic, the sign of  $(F_l^S - \bar{F}^S)$  is the same than

$$\langle s_l \rangle \left\langle \frac{1}{\sigma^{3/2}} \right\rangle - \left\langle \frac{1}{\sqrt{\sigma}} \right\rangle = \left\langle \frac{1}{\sqrt{\sigma}} \right\rangle \left( \frac{\langle s_l \rangle \langle 1/\sigma^{3/2} \rangle}{\langle 1/\sqrt{\sigma} \rangle} - 1 \right). \tag{18}$$

Since also  $\langle s_l \rangle > 0$ , we need to demonstrate that the following inequality always holds

$$\frac{\langle 1/\sigma^{3/2} \rangle}{\langle 1/\sqrt{\sigma} \rangle} \geq \left\langle \frac{1}{\sqrt{\sigma}} \right\rangle \frac{1}{\langle \sqrt{\sigma} \rangle}. \tag{19}$$

This can be proven from the chain of inequalities

$$\frac{\langle 1/\sigma^{3/2} \rangle}{\langle 1/\sqrt{\sigma} \rangle} \geq \left\langle \frac{1}{\sigma} \right\rangle \geq \left\langle \frac{1}{\sqrt{\sigma}} \right\rangle \left\langle \frac{1}{\sqrt{\sigma}} \right\rangle \geq \left\langle \frac{1}{\sqrt{\sigma}} \right\rangle \frac{1}{\langle \sqrt{\sigma} \rangle}. \tag{20}$$

In Eq. 20, the second and third inequalities are consequences of Jensen's inequality, since both  $x^2$  and  $1/x$  are convex functions. For the first inequality in Eq. 20, since  $s > 0$ , we can use the result  $\langle x^i \rangle \geq \langle x^j \rangle^{i/j}$  proved for  $i > j$  in [Kapur and Rani, 1995]. Combining this result for  $(i = 3, j = 2)$  and  $(i = 2, j = 1)$ , we obtain  $\langle x^3 \rangle \geq \langle x^2 \rangle \langle x \rangle$ . Taking  $\langle x \rangle = \langle 1/\sqrt{\sigma} \rangle$  we finally prove Eq. 20. Therefore, in the limit of small switching rates of the environment, the bet-hedging region is wider in the spatially varying case than in the temporally varying case.

In the opposite limit of high rates of environmental switch, the function to be optimized is linear, and the optimal strategy is a pure strategy. In this case, the particular phenotype  $l$  adopted by the whole population is that maximizing  $\sum_i p_i s_{il}$ . This conclusion holds both for temporally and spatially varying environments.

## 4 Conclusions

Understanding the precise mechanisms of population expansions is of utmost importance, not only for understanding species diversity, but also to cope with invasive species in new habitats [Wolf and Weissing, 2012, Sih et al., 2012, Chapple et al., 2012, Carere and Gherardi, 2013], bacterial infections [Frankel et al., 2014, Dufour et al., 2014, 2016, Jones and Lennon, 2010], and cell migration, such as those occurring during tissue renewal or cancer metastasis [Mayor and Etienne-Manneville, 2016]. Phenotypic diversity is a convenient strategy for the success of population expansions in a broad range of contexts [Wolf and Weissing, 2012, Sih et al., 2012, Chapple et al., 2012, Carere and Gherardi, 2013, Frankel et al., 2014, Dufour et al., 2014, 2016]. Although precise experimental measures are not easy to obtain, a recent study shows that populations with increased variability in individual risk-taking can colonize wider ranges of territories [Møller and Garamszegi, 2012].

In this work, we proposed a general mathematical and computational framework to analyze such scenarios. In particular, we introduced a population model with diverse phenotypes that perform differently depending on the type of environment. We focused on the “optimal” degree of diversity leading to the fastest average population expansion in an environment fluctuating either in space or in time. We found that, contrarily to the well-mixed case, bet-hedging can be convenient in expanding populations. This result complements the study in [Hidalgo et al., 2015] for a fixed habitat and supports the view that diversification is of broad importance for spatially-structured populations. For environments varying slowly in time, the expansion is relatively slow, and diverse communities can be optimal depending on the parameters. On the contrary, for fast environmental changes, the optimal population always adopts a unique strategy.

A remarkable outcome of our analysis is that spatial fluctuations create more opportunities for bet-hedging than temporal fluctuations, in that the region of parameter space where the optimal population is diverse, is always larger in the former case. One intuitive explanation is that in the case of spatial fluctuations, the population spends less time traversing favorable patches than adverse ones. This means that the beneficial effect of favorable patches is reduced with respect to the case of temporal fluctuations. Therefore, a pure risky strategy is less efficient in the case of spatial variability and can be more easily outcompeted by a diversified bet-hedging strategy.

The framework presented here can be extended to accommodate other scenarios. We have assumed that the fraction of individuals adopting each phenotype is fixed by the phenotypic switching rates. To understand the evolution of bet-hedging, it could be interesting to study scenarios in which the phenotypic switching rates are slower, so that phenotypes can be selected, and/or are themselves subject to evolution and selection [Xue and Leibler, 2016, Hufton et al., 2018]. Another potentially relevant extension would be to consider two-dimensional habitats. Although the classic theory for Fisher waves [Fisher, 1937, Kolmogorov et al., 1937] is unaffected in higher dimensions, in the presence of spatial heterogeneity the front shape can become anisotropic, potentially affecting the results. Similarly, it would be interesting to analyze the combined effect of spatial and temporal variability. We also limited ourselves to the case where the different environments affect individual growth rates, whereas in general, one could also expect them to have an effect on motility [Shigesada et al., 1979, 1986, Pigolotti and Benzi, 2014, 2016, Gueudré et al., 2014], opening the way for different forms of bet-hedging. Finally, the present study was limited to pulled waves. It would be interesting to study the effect of bet-hedging on pushed waves, for example to describe population expansion in the presence of an Allee effect [Gandhi et al., 2016, Birzu et al., 2018].

It would be also interesting to experimentally test our results. Experiments of expanding bacterial colonies in non-homogeneous environments have already been performed and shed light, for example, on the evolution of antibiotic resistance in spatially-structured populations [Baym et al., 2016]. To perform experiments within the limits of our theory, a challenge can be to maintain the environmental variability sufficiently low to avoid exposing the population to an excessive evolutionary pressure. Similar problems appear, for example, in studies of range expansion of mutualistic bacteria [Müller et al., 2014]. An extension of the theory including both phenotypic and genetic diversity could account for these scenarios.

In summary, we have introduced a model to understand conditions favoring diversification of an expanding population. Our work provides a bridge between the theory of bet-hedging and that of ecological range expansion described by reaction-diffusion equations. The results of the model highlight the relation between population diversity and fluctuations of the environment encountered during range expansion. The flexibility and generality of our framework make it a useful starting point for applications to a wide range of ecological scenarios.

## 5 Acknowledgments

We acknowledge Steven D. Aird, R. Rubio de Casas, and Massimo Cencini for comments on a preliminary version of this manuscript. MAM is grateful to the Spanish-MINECO/AEIa for financial support (under grant ref. FIS2017-84256-P; FEDER funds).

## 6 Supporting information

### 6.1 Numerical integration of the stochastic Fisher equation

In this section we describe in detail the methods applied for the integration of the wave equations of the two-phenotype model studied in the Main Text.

#### 6.1.1 Fisher wave

We consider the Fisher equation

$$\dot{f}(x, t) = D\nabla^2 f(x, t) + \sigma(x, t)f(x, t)(1 - f(x, t)), \quad (21)$$

where  $f(x, t)$  is the population density at space  $x$  and time  $t$ , and  $\sigma(x, t)$  is the local growth rate.

We employ a finite-difference fourth-order Runge-Kutta method. The systems is initialized by fixing  $f(x_i, 0) = 1$  for  $i \in (0, 50)$  and  $f(x, t) = 0$  for  $i > 50$ . To fix  $dx$ , we implement an adaptive routine. We initialize the routine with an initial guess for  $dx = 0.14$ . Then

1. We let the system evolve until the front reaches a stationary state.
2. We compute the smallest values of  $x$  for which  $f(x, t) > \theta$  for  $\theta = 3/4$  and  $\theta = 1/4$ . We denote these two values as  $x_{3/4}$  and  $x_{1/4}$  respectively.
3. We measure the precisions  $\Delta f_{3/4} = f(x_{3/4} - dx) - f(x_{3/4})$ ,  $\Delta f_{1/4} = f(x_{1/4} - dx) - f(x_{1/4})$ .
4. If  $\Delta f_{3/4} > 0.01$  and  $\Delta f_{1/4} > 0.01$ , then  $dx$  is a valid increment.
5. Otherwise, the system is set to the initial conditions and the routine is again run for  $dx = d\tilde{x} - 0.01$ ; being  $d\tilde{x}$  the previously employed increment.

Once  $dx$  is selected,  $dt$  is fixed following the Courant–Friedrichs–Lewy condition for an explicit integration method [Courant et al., 1967]:

$$\frac{v_{\max} dt}{dx} \leq 1 \quad (22)$$

being  $v_{\max}$  the estimated maximum velocity of the wave. We fix  $v_{\max} = 100$ , which is an overestimation of the maximum velocity in our simulations.

Temporal environmental switch is numerically implemented with a simple first-order algorithm. At the beginning of each time step, the state of environment is switched with probability  $k dt$ . We verified that this quantity is always sufficiently small, so that the first-order algorithm yields reliable results. A similar algorithm is implemented for spatial environmental variations to sequentially assign an environmental state to each lattice site.

#### 6.1.2 Stochastic Fisher wave

We consider the stochastic Fisher equation [Korolev et al., 2010]

$$\dot{f}(x, t) = D\nabla^2 f + \sigma(t)f(1 - f) + \sqrt{\frac{2}{N}}f(1 - f)\xi(x, t) \quad (23)$$

where  $\xi(x, t)$  a Gaussian white noise satisfying  $\langle \xi(x, t) \rangle = 0$  and  $\langle \xi(x, t)\xi(x', t') \rangle = \delta(x - x')\delta(t - t')$ .

Numerical integration in the presence of noise is subtle. In particular, one has to figure out how to deal with the unphysical values  $f(x, t) < 0$  and  $f(x, t) > 1$  obtained numerically. In some parameter range, the naive replacement  $f(x, t) = 0$  or  $f(x, t) = 1$  when  $f(x, t) < 0$  and  $f(x, t) > 1$ , respectively, introduces a bias that can profoundly alter the results. In particular, an incorrect integration of  $f(x, t)$  at the front, where  $f(x, t)$  is small, might lead to a large error in the estimated velocity. However, when  $f(x, t)$  is small so that  $\gamma(t) \simeq \sqrt{\frac{2}{N}f(t)}$ , this problem can be circumvented by integrating the noise term exactly [Dornic et al., 2005].

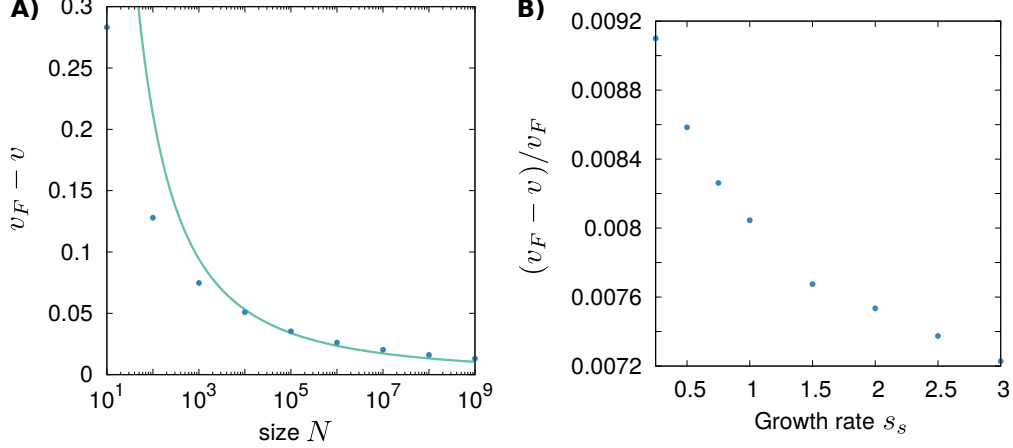


Figure 6: **Size scaling and maximum error estimation for our integration method.** Panel A) shows the curve  $4.5 \log N^{-2}$  and the difference  $v_F - v$  for  $k = 0$ ,  $\alpha = 0$ ,  $s_s = 1$ , and different system sizes. Panel B) shows  $(v_F - v)/v_F$  for  $N = 10^9$  and different growth rates employed in this work. These results suggest that our integration method is precise and have a maximum error of 0.0018%.

Taking this into account, we integrate the equation mixing two different algorithms, depending on the local value of  $f(x, t)$ :

- If  $f(x, t) > \theta$ : we employ the Milstein method (order 1). Defining  $\beta(t) \equiv D\nabla^2 f(t) + \sigma(t)f(t)(1 - f(t))$  and  $\gamma(t) \equiv \sqrt{\frac{2}{N}f(t)(1 - f(t))}$ , the local field is updated according to the rule

$$f(x, t + dt) = f(x, t) + \beta(t)dt + \gamma(t)\Delta + \frac{1}{2}\gamma(t)\frac{\partial\gamma}{\partial f(t)}(\Delta^2 - dt) \quad (24)$$

being  $\Delta = \sqrt{dt}N(0, 1)$ .

- If  $f(x, t) < \theta$ : we perform the two-step numerical integration proposed in [Dornic et al., 2005]:
  1. *Non-linear and diffusion terms.* Integration of  $\dot{f}(x, t) = D\nabla^2 f - \sigma(t)f^2$  is done by employing the Runge-Kutta method obtaining a first solution  $f^*$ .
  2. *Linear and stochastic terms.* The term  $\sigma(t)f + \sqrt{\frac{2}{N}f\xi(x, t)}$  is integrated in an exact way as [Dornic et al., 2005]:

$$f(x, t) = r_{\text{Gamma}}\{r_{\text{Poisson}}\{\lambda f^*(x, t)e^{\sigma(t)t}\}\}/\lambda. \quad (25)$$

being  $\lambda = \frac{2\sigma(t)}{\gamma^2 e^{\sigma(t)t}}$ , and  $r_{\text{Gamma}}, r_{\text{Poisson}}$  random values obtained from the Gamma and Poisson probability distributions, i.e.  $\text{Prob}[r_{\text{Gamma}}(a) = z] = \frac{z^{a-1}e^{-z}}{\Gamma[a]}$  and  $\text{Prob}[r_{\text{Poisson}}(a) = z] = \frac{a^z e^{-a}}{z!}$ , respectively.

To check the precision of our method we integrated the stochastic equation 23 for  $k = 0$ ,  $\alpha = 0$ , and different growth rates  $s_s$  and compared the results to the analytical Fisher velocity  $v_F = 2\sqrt{Ds_s}$ . For large population size  $N$ , the velocity  $v$  of the wave asymptotically goes as  $v_F - v \simeq C \ln^{-2}(N)$  [Brunet and Derrida, 2001]. Our numerical integration is consistent with this asymptotic relation from  $N \simeq 10^4$  (figure 6A) with a root-mean-square deviation of 0.002. We have also obtained the values  $(v_F - v)/v_F$  for the different growth rates employed in this work to obtain an estimation of the maximum error we expect (see figure 6B). Note that  $v_F$  is not the actual velocity the finite system is expected to reach, so the relative error  $(v_F - v)/v_F$  is, in fact, smaller. The maximum error value is around 0.9%, that, considering the results of figure 6A) leads to an overestimated error of about 0.0018%.

## 6.2 Effect of finite population size for spatially varying environments

Analogously to the temporally varying case (Section 3.1.5), we study the effect of demographic stochasticity induced by the finite size of the population for spatially varying environments. In this case, the corresponding stochastic Fisher wave is described by the equation

$$\dot{f}(x, t) = D\nabla^2 f + \sigma(x)f(1-f) + \sqrt{\frac{2}{N}}f(1-f)\xi(x, t), \quad (26)$$

analogous to Eq. 10 of Section 3.1.5. Following the procedure described in this Supplementary Material, we numerically integrated this equation. In this case, stochasticity slightly alters the deterministic prediction (see Fig. 7). Specifically, the asymptotic mean velocities  $v_M$  decay slightly faster with the fraction of risky individuals  $\alpha$ . This implies that parameters at which an optimal  $\alpha^* = 1$  is reached at the deterministic approach, lead to a bet-hedging strategy with  $\alpha^* < 1$  in the stochastic system. As the lower limit for stochastic systems must still be the deterministic one,  $\tilde{s}_b > 2 - \tilde{s}_a$ , bet-hedging region is then slightly enlarged for finite size populations in spatially varying environments.

Despite this slight difference between the deterministic and stochastic systems, the main predictions described for spatially varying environments in the main text are still maintained.

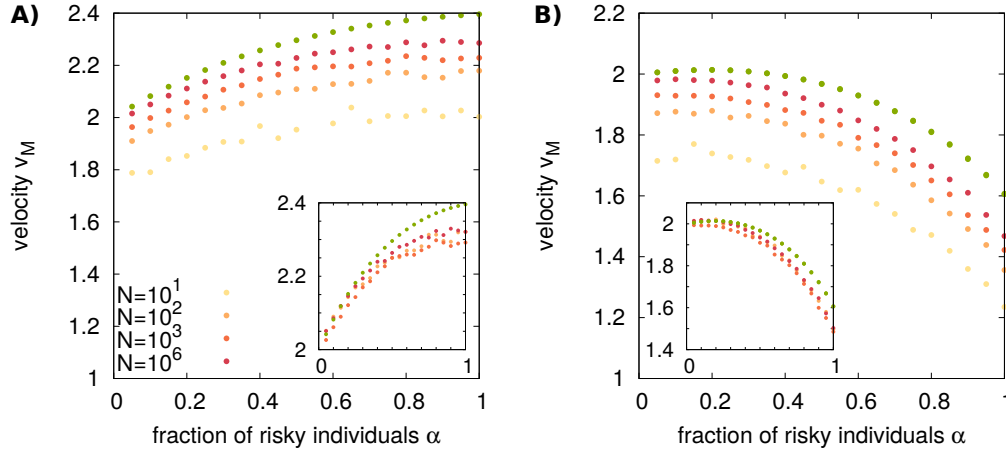


Figure 7: **Optimal strategy with fluctuations induced by finite population size in spatially varying environments.** (A) Asymptotic mean velocities obtained by numerical integration of the stochastic Fisher (26) for  $\tilde{s}_a = 0.75$ ,  $s_s = 0.01$ ,  $\tilde{s}_b = 3$  (yellow dot of Fig. 4) and different population sizes, shown in the figure legend. (B) Same for  $\tilde{s}_a = 0.25$ ,  $s_s = 1$ ,  $\tilde{s}_b = 2$  (blue dot of Fig. 4). In both panels, the temporal switching rate of the environment is  $k = 0.001$ . Green dots corresponds to the results of the deterministic approach (Eq. 5) for  $k = 0.001$ . Insets show a collapse of the curves according to Eq. 11, with a fitted value of  $C = 3$ .

## References

- Peter Ashcroft, Philipp M Altrock, and Tobias Galla. Fixation in finite populations evolving in fluctuating environments. *Journal of The Royal Society Interface*, 11(100):20140663, 2014.
- KA Bartoń, T Hovestadt, BL Phillips, and JM Travis. Risky movement increases the rate of range expansion. *Proceedings of the Royal Society of London B: Biological Sciences*, 279(1731):1194–1202, 2012.
- Michael Baym, Tami D Lieberman, Eric D Kelsic, Remy Chait, Rotem Gross, Idan Yelin, and Roy Kishony. Spatiotemporal microbial evolution on antibiotic landscapes. *Science*, 353(6304):1147–1151, 2016.
- Eshel Ben-Jacob, Inon Cohen, and Herbert Levine. Cooperative self-organization of microorganisms. *Advances in Physics*, 49(4):395–554, 2000.
- Gabriel Birzu, Oskar Hallatschek, and Kirill S Korolev. Fluctuations uncover a distinct class of traveling waves. *Proceedings of the National Academy of Sciences*, 115(16):E3645–E3654, 2018.
- Éric Brunet and Bernard Derrida. Effect of microscopic noise on front propagation. *Journal of Statistical Physics*, 103(1-2):269–282, 2001.

- Claudio Carere and Francesca Gherardi. Animal personalities matter for biological invasions. *Trends in ecology & evolution*, 28(1):5–6, 2013.
- Massimo Cencini, Cristobal Lopez, and Davide Vergni. Reaction-diffusion systems: front propagation and spatial structures. In *The Kolmogorov Legacy in Physics*, pages 187–210. Springer, 2003.
- David G Chapple, Sarah M Simmonds, and Bob BM Wong. Can behavioral and personality traits influence the success of unintentional species introductions? *Trends in Ecology & Evolution*, 27(1):57–64, 2012.
- Dylan Z Childs, CJE Metcalf, and Mark Rees. Evolutionary bet-hedging in the real world: empirical evidence and challenges revealed by plants. *Proceedings of the Royal Society of London B: Biological Sciences*, page rspb20100707, 2010.
- Hugh N Comins, William D Hamilton, and Robert M May. Evolutionarily stable dispersal strategies. *Journal of theoretical Biology*, 82(2):205–230, 1980.
- Richard Courant, Kurt Friedrichs, and Hans Lewy. On the partial difference equations of mathematical physics. *IBM journal of Research and Development*, 11(2):215–234, 1967.
- Imke G de Jong, Patsy Haccou, and Oscar P Kuipers. Bet hedging or not? a guide to proper classification of microbial survival strategies. *Bioessays*, 33(3):215–223, 2011.
- Pieter J Den Boer. Spreading of risk and stabilization of animal numbers. *Acta biotheoretica*, 18(1-4):165–194, 1968.
- Sebastian Dewhurst and Frithjof Lutscher. Dispersal in heterogeneous habitats: thresholds, spatial scales, and approximate rates of spread. *Ecology*, 90(5):1338–1345, 2009.
- Ivan Dornic, Hugues Chaté, and Miguel A Munoz. Integration of langevin equations with multiplicative noise and the viability of field theories for absorbing phase transitions. *Physical review letters*, 94(10):100601, 2005.
- Renée A Duckworth. Adaptive dispersal strategies and the dynamics of a range expansion. *The American Naturalist*, 172(S1):S4–S17, 2008.
- Yann S Dufour, Xiongfei Fu, Luis Hernandez-Nunez, and Thierry Emonet. Limits of feedback control in bacterial chemotaxis. *PLoS computational biology*, 10(6):e1003694, 2014.
- Yann S Dufour, Sébastien Gillet, Nicholas W Frankel, Douglas B Weibel, and Thierry Emonet. Direct correlation between motile behavior and protein abundance in single cells. *PLoS computational biology*, 12(9):e1005041, 2016.
- Casimir Emako, Charlène Gayraud, Axel Buguin, Luís Neves de Almeida, and Nicolas Vauchelet. Traveling pulses for a two-species chemotaxis model. *PLoS computational biology*, 12(4):e1004843, 2016.
- Robert Fernholz and Brian Shay. Stochastic portfolio theory and stock market equilibrium. *The Journal of Finance*, 37(2):615–624, 1982.
- Ronald Aylmer Fisher. The wave of advance of advantageous genes. *Annals of Human Genetics*, 7(4):355–369, 1937.
- Sean Fogarty, Julien Cote, and Andrew Sih. Social personality polymorphism and the spread of invasive species: a model. *The American Naturalist*, 177(3):273–287, 2011.
- Nicholas W Frankel, William Pontius, Yann S Dufour, Junjiajia Long, Luis Hernandez-Nunez, and Thierry Emonet. Adaptability of non-genetic diversity in bacterial chemotaxis. *Elife*, 3:e03526, 2014.
- Xiongfei Fu, Setsu Kato, Junjiajia Long, Henry H Mattingly, Caiyun He, Dervis Can Vural, Steven W Zucker, and Thierry Emonet. Spatial self-organization resolves conflicts between individuality and collective migration. *Nature communications*, 9(1):2177, 2018.
- Saurabh R Gandhi, Eugene Anatoly Yurtsev, Kirill S Korolev, and Jeff Gore. Range expansions transition from pulled to pushed waves as growth becomes more cooperative in an experimental microbial population. *Proceedings of the National Academy of Sciences*, 113(25):6922–6927, 2016.
- Thomas Gueudré, Alexander Dobrinevski, and Jean-Philippe Bouchaud. Explore or exploit? a generic model and an exactly solvable case. *Physical review letters*, 112(5):050602, 2014.
- Oskar Hallatschek and David R Nelson. Gene surfing in expanding populations. *Theoretical population biology*, 73(1):158–170, 2008.

- Oskar Hallatschek, Pascal Hersen, Sharad Ramanathan, and David R Nelson. Genetic drift at expanding frontiers promotes gene segregation. *Proceedings of the National Academy of Sciences*, 104(50):19926–19930, 2007.
- William D Hamilton and Robert M May. Dispersal in stable habitats. *Nature*, 269(5629):578, 1977.
- Gregory P Harmer and Derek Abbott. Game theory: Losing strategies can win by parrondo’s paradox. *Nature*, 402(6764):864, 1999.
- Alan Hastings, Kim Cuddington, Kendi F Davies, Christopher J Dugaw, Sarah Elmendorf, Amy Freestone, Susan Harrison, Matthew Holland, John Lambrinos, Urmila Malvadkar, et al. The spatial spread of invasions: new developments in theory and evidence. *Ecology Letters*, 8(1):91–101, 2005.
- Jorge Hidalgo, Simone Pigolotti, and Miguel A Munoz. Stochasticity enhances the gaining of bet-hedging strategies in contact-process-like dynamics. *Physical Review E*, 91(3):032114, 2015.
- Jorge Hidalgo, Rafael Rubio de Casas, and Miguel Á Muñoz. Environmental unpredictability and inbreeding depression select for mixed dispersal syndromes. *BMC evolutionary biology*, 16(1):71, 2016.
- Josef Hofbauer and Karl Sigmund. *Evolutionary games and population dynamics*. Cambridge university press, 1998.
- Keith R Hopper. Risk-spreading and bet-hedging in insect population biology. *Annual review of entomology*, 44(1):535–560, 1999.
- Peter G Hufton, Yen Ting Lin, Tobias Galla, and Alan J McKane. Intrinsic noise in systems with switching environments. *Physical Review E*, 93(5):052119, 2016.
- Peter G Hufton, Yen Ting Lin, and Tobias Galla. Phenotypic switching of populations of cells in a stochastic environment. *Journal of Statistical Mechanics: Theory and Experiment*, 2018(2):023501, 2018.
- Vincent AA Jansen and Jin Yoshimura. Populations can persist in an environment consisting of sink habitats only. *Proceedings of the National Academy of Sciences*, 95(7):3696–3698, 1998.
- Stuart E Jones and Jay T Lennon. Dormancy contributes to the maintenance of microbial diversity. *Proceedings of the National Academy of Sciences*, 107(13):5881–5886, 2010.
- JN Kapur and Anju Rani. Testing the consistency of given values of a set of moments of a probability distribution. *J. Bihar Math. Soc.*, 16:51–63, 1995.
- Evelyn F Keller and Lee A Segel. Traveling bands of chemotactic bacteria: a theoretical analysis. *Journal of theoretical biology*, 30(2):235–248, 1971.
- John L Kelly Jr. A new interpretation of information rate. In *The Kelly Capital Growth Investment Criterion: Theory and Practice*, pages 25–34. World Scientific, 2011.
- AN Kolmogorov, IG Petrovskii, and NS Piskunov. A study of the diffusion equation with increase in the amount of substance, and its application to a biological problem. *Selected Works of AN Kolmogorov I*, pages 248–270, 1937.
- Kirill S Korolev, Mikkel Avlund, Oskar Hallatschek, and David R Nelson. Genetic demixing and evolution in linear stepping stone models. *Reviews of modern physics*, 82(2):1691, 2010.
- Edo Kussell and Stanislas Leibler. Phenotypic diversity, population growth, and information in fluctuating environments. *Science*, 309(5743):2075–2078, 2005.
- Tai-Chia Lin and Zhi-An Wang. Development of traveling waves in an interacting two-species chemotaxis model. *Discrete Continuous Dynamical Systems Series A*, 34(7):2907–2927, 2014.
- Roberto Mayor and Sandrine Etienne-Manneville. The front and rear of collective cell migration. *Nature reviews Molecular cell biology*, 17(2):97, 2016.
- Anders Pape Møller and László Zsolt Garamszegi. Between individual variation in risk-taking behavior and its life history consequences. *Behavioral Ecology*, 23(4):843–853, 2012.
- Esteban Moro. Internal fluctuations effects on fisher waves. *Physical Review Letters*, 87(23):238303, 2001.
- Esteban Moro. Numerical schemes for continuum models of reaction-diffusion systems subject to internal noise. *Physical Review E*, 70(4):045102, 2004.

- Melanie JI Müller, Beverly I Neugeboren, David R Nelson, and Andrew W Murray. Genetic drift opposes mutualism during spatial population expansion. *Proceedings of the National Academy of Sciences*, 111(3):1037–1042, 2014.
- Michael G Neubert and Hal Caswell. Demography and dispersal: calculation and sensitivity analysis of invasion speed for structured populations. *Ecology*, 81(6):1613–1628, 2000.
- Martin A Nowak. *Evolutionary dynamics*. Harvard University Press, 2006.
- Juan MR Parrondo, Gregory P Harmer, and Derek Abbott. New paradoxical games based on brownian ratchets. *Physical Review Letters*, 85(24):5226, 2000.
- Simone Pigolotti and Roberto Benzi. Selective advantage of diffusing faster. *Physical review letters*, 112(18):188102, 2014.
- Simone Pigolotti and Roberto Benzi. Competition between fast-and slow-diffusing species in non-homogeneous environments. *Journal of theoretical biology*, 395:204–210, 2016.
- E Rajon, S Venner, and F Menu. Spatially heterogeneous stochasticity and the adaptive diversification of dormancy. *Journal of evolutionary biology*, 22(10):2094–2103, 2009.
- Sohini Ramachandran, Omkar Deshpande, Charles C Roseman, Noah A Rosenberg, Marcus W Feldman, and L Luca Cavalli-Sforza. Support from the relationship of genetic and geographic distance in human populations for a serial founder effect originating in africa. *Proceedings of the National Academy of Sciences of the United States of America*, 102(44):15942–15947, 2005.
- Igor M Rouzine, Ariel D Weinberger, and Leor S Weinberger. An evolutionary role for hiv latency in enhancing viral transmission. *Cell*, 160(5):1002–1012, 2015.
- Sebastian J Schreiber and James O Lloyd-Smith. Invasion dynamics in spatially heterogeneous environments. *The American Naturalist*, 174(4):490–505, 2009.
- Nanako Shigesada and Kohkichi Kawasaki. *Biological invasions: theory and practice*. Oxford University Press, UK, 1997.
- Nanako Shigesada, Kohkichi Kawasaki, and Ei Teramoto. Spatial segregation of interacting species. *Journal of Theoretical Biology*, 79(1):83–99, 1979.
- Nanako Shigesada, Kohkichi Kawasaki, and Ei Teramoto. Traveling periodic waves in heterogeneous environments. *Theoretical Population Biology*, 30(1):143–160, 1986.
- Andrew Sih, Julien Cote, Mara Evans, Sean Fogarty, and Jonathan Pruitt. Ecological implications of behavioural syndromes. *Ecology letters*, 15(3):278–289, 2012.
- John Maynard Smith. Evolution and the theory of games. In *Did Darwin Get It Right?*, pages 202–215. Springer, 1988.
- Ana Solopova, Jordi van Gestel, Franz J Weissing, Herwig Bachmann, Bas Teusink, Jan Kok, and Oscar P Kuipers. Bet-hedging during bacterial diauxic shift. *Proceedings of the National Academy of Sciences*, 111(20):7427–7432, 2014.
- Michael PH Stumpf, Zoë Laidlaw, and Vincent AA Jansen. Herpes viruses hedge their bets. *Proceedings of the National Academy of Sciences*, 99(23):15234–15237, 2002.
- Wim Van Saarloos. Front propagation into unstable states. *Physics reports*, 386(2-6):29–222, 2003.
- Jan-Willem Veening, Wiep Klaas Smits, and Oscar P Kuipers. Bistability, epigenetics, and bet-hedging in bacteria. *Annu. Rev. Microbiol.*, 62:193–210, 2008.
- Jonathan M Waters, Ceridwen I Fraser, and Godfrey M Hewitt. Founder takes all: density-dependent processes structure biodiversity. *Trends in ecology & evolution*, 28(2):78–85, 2013.
- Paul David Williams and Alan Hastings. Paradoxical persistence through mixed-system dynamics: towards a unified perspective of reversal behaviours in evolutionary ecology. *Proceedings of the Royal Society of London B: Biological Sciences*, page rspb20102074, 2011.
- Denise M Wolf, Vijay V Vazirani, and Adam P Arkin. Diversity in times of adversity: probabilistic strategies in microbial survival games. *Journal of theoretical biology*, 234(2):227–253, 2005a.



Denise M Wolf, Vijay V Vazirani, and Adam P Arkin. A microbial modified prisoner's dilemma game: how frequency-dependent selection can lead to random phase variation. *Journal of theoretical biology*, 234(2):255–262, 2005b.

Max Wolf and Franz J Weissing. Animal personalities: consequences for ecology and evolution. *Trends in ecology & evolution*, 27(8):452–461, 2012.

Alan J Wolfe and Howard C Berg. Migration of bacteria in semisolid agar. *Proceedings of the National Academy of Sciences*, 86(18):6973–6977, 1989.

BingKan Xue and Stanislas Leibler. Evolutionary learning of adaptation to varying environments through a transgenerational feedback. *Proceedings of the National Academy of Sciences*, 113(40):11266–11271, 2016.